First-order transitions in anisotropic magnets with random fields and random uniaxial anisotropies

Yadin Y. Goldschmidt
Department of Physics and Astronomy, University of Pittsburgh, Pittsburgh, Pennsylvania 15260

Amnon Aharony
School of Physics and Astronomy, Tel Aviv University, Tel Aviv 69978, Israel
(Received 11 March 1985)

Long-range magnetic order is known to be replaced by a spin-glass phase for rotationally invariant N-component spin systems with random fields or random uniaxial anisotropies. Using exact calculations in the limit $N\to\infty$, we show how long-range order is restored when a uniform anisotropy is added. For a uniaxial anisotropy g, long-range order is achieved above a critical value of g, at which a phase with an infinite susceptibility occurs. For higher-order (e.g., cubic or hexagonal) anisotropies long-range order is reached via first-order transitions. Scaling arguments and explicit calculations are used to obtain detailed predictions on the shape of the various phase boundaries.

I. INTRODUCTION

When fluctuations are taken into account, various types of random quenched interactions destroy long-range ferromagnetic (FM) order in Heisenberg-like *isotropic* (N-component) spin systems with realistic dimensionalities $d<4$. Of particular interest are systems with *random magnetic fields,*[1] where the randomness enters via

$$\mathscr{H}_h=\sum_x \mathbf{h}(x)\cdot\mathbf{S}(x)\ , \tag{1.1}$$

$\mathbf{S}(x)$ being the N-component spin vector at site x, while $\mathbf{h}(x)$ is the random field, with configurational averages

$$[\mathbf{h}(x)]_{\rm av}=0,\quad [\,|\mathbf{h}(x)|^2]_{\rm av}=\Delta_F \tag{1.2}$$

or systems with *random uniaxial anisotropies,*[2] with, e.g.,

$$\mathscr{H}_a=-\sum_x [\mathbf{a}(x)\cdot\mathbf{S}(x)]^2\ , \tag{1.3}$$

where

$$[\mathbf{a}(x)]_{\rm av}=0,\quad [\,|\mathbf{a}(x)|^2]_{\rm av}=w\ . \tag{1.4}$$

Systems with *random off-diagonal exchange interactions,*[3]

$$\mathscr{H}_r=\sum_{x,x'}\sum_{i,j} J_{ij}(x,x')S^i(x)S^j(x') \tag{1.5}$$

($i,j=1,\ldots,N$ are the spin-component indices) which result, e.g., from dipole-dipole interactions, random quenched strains, spin-orbit interactions, Dzyaloshinskii-Moriya interactions, etc., are expected to exhibit the same properties as those with random uniaxial anisotropies.

The absence of long-range order in these systems can be shown by a perturbative expansion (in Δ_F or in w). Assuming a net magnetization $\mathbf{M}$, the fluctuations in the transverse spin components $[\langle S_\perp(x)\rangle^2]_{\rm av}$ are shown to be proportional (to leading order in Δ_F or in w^2M^2) to

$$\int \frac{d^dp}{(p^2+r_T)^2}\propto r_T^{(d-4)/2}\ , \tag{1.6}$$

and thus to diverge for $d<4$ as the inverse-transverse susceptibility $r_T=H/M$ vanishes with the magnetic field H.[1,2,3]

A similar lowest-order expansion of the *equation of state* also shows no solution with $M\neq 0$ as $H\to 0$.[4] However, it is difficult in general to sum this expansion to all orders and to identify the phases that replace the FM one. Such a summation *is* possible in the limit $N\to\infty$. For the random-field (RF) case this has already been done in the original paper by Lacour-Gayet and Toulouse.[5] For $d<4$, any finite value of Δ_F yields spin-glass (SG) ordering,[6] with a finite Edwards-Anderson[7] order parameter

$$q=[\langle\mathbf{S}\rangle^2]_{\rm av} \tag{1.7}$$

at all temperatures. For $d>4$, the SG phase is replaced by a FM one (with q also nonzero) for sufficiently small T and Δ_F. The relevant phase diagrams are shown in Figs. 1(a) and 1(b).

The summation to all orders in w, for the random-anisotropy (RA) case, is possible for large N if the large-N behavior of w is given by[8] $w^2=\Delta_A/(4!N)$. For $d<4$, one again finds a SG phase for all finite values of Δ_A,

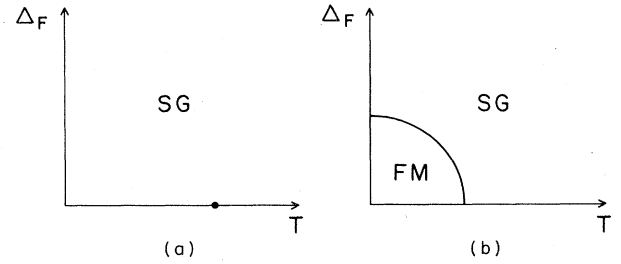

FIG. 1. (a) Phase diagram for the random-field case below four dimensions. The black dot is the location of the critical temperature for $\Delta_F=0$. (b) Phase diagram for the random-field case above four dimensions. FM denotes a ferromagnetic phase and SG a spin-glass phase.

which undergoes a second-order transition into the paramagnetic (PM) phase at high temperatures [Fig. 2(a)]. For $d>4$, one again recovers the FM phase [Fig. 2(b)].

As already pointed out in Ref. 3, real crystals never obey the rotational invariance needed for deriving the above results. In particular, real systems may have *cubic anisotropies,*[9]

$$\mathscr{H}_4=-\frac{v_4}{4N}\sum_x\sum_{i=1}^{N}[S^i(x)]^4\,, \tag{1.8}$$

hexagonal ones,[10]

$$\mathscr{H}_6=-\frac{v_6}{6N^2}\sum_x\sum_i[S^i(x)]^6\,, \tag{1.9}$$

etc. One may also encounter weak *uniaxial anisotropies,*[11]

$$\mathscr{H}_g=g\sum_x\left[\frac{1}{N}\sum_{i=2}^{N}[S^i(x)]^2-\frac{N-1}{N}[S^1(x)]^2\right], \tag{1.10}$$

which prefer ordering of the S^1 component if $g>0$. In all of these anisotropic cases, rotational invariance is broken. At low temperatures, the transverse "mass" r_T is finite, the integral in Eq. (1.6) does not diverge, and FM long-range order may be restored. It was conjectured in Ref. 3 that this FM order would appear at low temperatures via a *first-order transition* [for (1.8) and (1.9)]. This was supported by the absence of physically stable and accessible fixed points in $d=4-\epsilon$ dimensions.[12,13] However, it was never explicitly confirmed in a detailed calculation. The present paper presents such a confirmation via explicit calculations in the limit $N\to\infty$.

Since the detailed calculations are somewhat technical, we start in Sec. II with a qualitative description of the results, including a discussion of the Arrott plots[14] for the equation of state and of the new predicted phase diagrams. We then proceed in Sec. III with a discussion of the ground state, extending the Imry-Ma[1] and the zero-temperature scaling arguments to show that strong anisotropies will restore FM long-range order and to estimate the threshold for this SG→FM transition. Section IV then contains a general scaling analysis, yielding the shapes of the predicted phase diagrams in terms of the relevant crossover exponents. The main calculational parts of the paper are described in Sec. V, where the general equation of state is calculated for $N\to\infty$, and in Sec. VI, where the example of cubic systems with random uniaxial anisotropies is treated in detail. Section VII then reviews the other cases, and Sec. VIII summarizes our conclusions and discusses relevant experiments.

II. QUALITATIVE DESCRIPTION OF RESULTS

A convenient way to analyze experimental results on the equation-of-state uses Arrott plots,[14] in which M^2 is plotted against H/M at fixed temperature T. Reference 8 gives this function explicitly for $N\to\infty$ as

$$M^2=f(T,H/M)\,. \tag{2.1}$$

The Arrott plots for the RF case in $d<4$ and for the RA case are plotted in Figs. 3(a) and 3(b), respectively.[15] In both cases, there is no intercept of an isotherm with the M^2 axis and thus no spontaneous magnetization at $H=0$.

The only change that we find (for $N\to\infty$) when we introduce anisotropy into the system is that H/M in Eq. (2.1) must be replaced by a modified transverse-inverse susceptibility r_T, which is particularly simple in the limit $N\to\infty$. For the uniaxial anisotropy (1.10), r_T is simply given by

$$r_T=H/M+g\,. \tag{2.2}$$

Thus, the Arrott plots of Fig. 3 are simply shifted to the left, $H/M\to H/M-g$, and a ferromagnetic phase appears for large enough g when the M^2 axis starts crossing isotherms. In the RF case, Fig. 1(a) turns into Fig. 4(a): At any finite g, the Δ_F-T diagram looks like Fig. 1(b), while at finite Δ_F the g-T diagram is shown in Fig. 5(a). Similarly, Fig. 2(a) turns, in the RA case, into Fig. 4(b): At finite g one expects Fig. 2(b), and at finite Δ_A one expects Fig. 5(b).

It is interesting to note that in the RA case, the point $g=\Sigma_c$ is a very special one: At this point all the low-temperature Arrott plots approach the origin with infinite slope, and one recovers a whole low-temperature phase with infinite longitudinal susceptibility (the transverse susceptibility is finite and equal to g). This is the phase predicted in Ref. 4 that now emerges even after all the orders in Δ_A have been taken into account. Of course, this is not surprising since the line $g=\Sigma_c$ is just the phase boundary between the spin-glass and the ferromagnetic phases. Since this transition turns out to be of second order the susceptibility diverges. When N is not infinite this line may not correspond to points of equal g, i.e., it can be

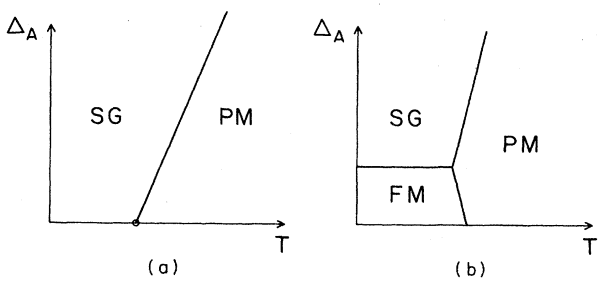

FIG. 2. (a) Phase diagram for the random-axis model below four dimensions. PM refers to a paramagnetic phase. (b) Same as (a) for $d>4$.

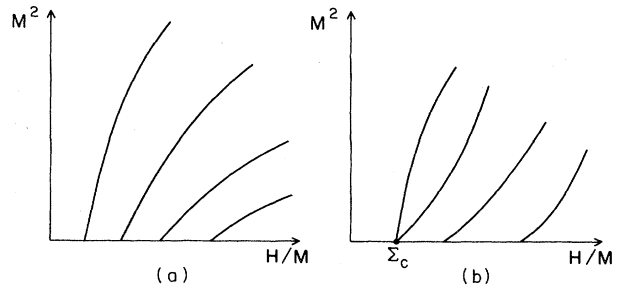

FIG. 3. (a) Arrott plots for the random-field case, $\Delta_F>0$. (b) Arrott plots for the random-anisotropy case, $\Delta_A>0$. Σ_c denotes the value of the transverse mass below the transition.

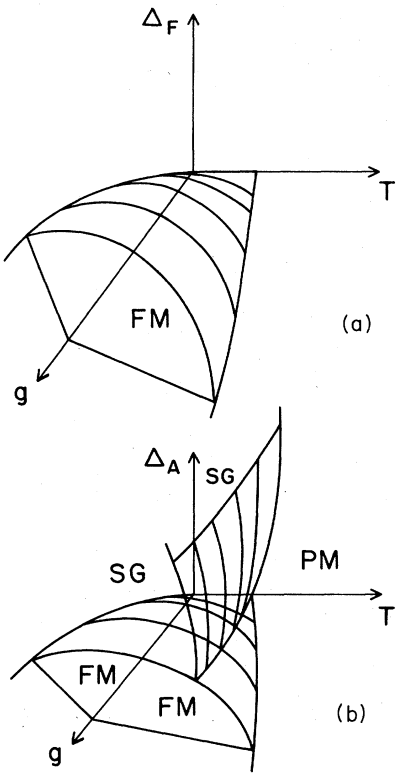

FIG. 4. (a) Three-dimensional phase diagram for the random-field case in the presence of a quadratic anisotropy. Similar phase diagram applies to the case of a cubic anisotropy. (b) Three-dimensional phase diagram for the random anisotropy in the presence of a quadratic anisotropy.

described by some function $g(T)$. Still, we expect the susceptibility to diverge along this line. The exponents are expected to be those of the Ising model in a random field, which at least in perturbation theory are given by the mapping $d \to d-2$ (this is because since $q \neq 0$ on this line there is an effective random field in the system even in the RA case as discussed, e.g., in Ref. 8).

For the cubic anisotropy (1.8), we find for $N \to \infty$,

$$r_T = H/M + v_4 M^2 \tag{2.3}$$

and the equation satisfied by r_T ($\equiv \Sigma$, the self-energy in the large-N limit, since in that case Σ is momentum independent) remains unchanged. This means that an Arrott plot of M^2 vs H/M in the case $v_4 > 0$ can be easily obtained from the plot of $y = M^2$ vs $x = \Sigma$ (which is the Arrott plot in the $v_4 = 0$ case). This is achieved by a simple rotation of the x axis by an angle θ satisfying $\tan\theta = -v_4$. The situation is explained in Fig. 6. We call the rotated axis the X axis. In order to find the value of H/M corresponding to a given point (M^2, Σ) in the M^2 vs Σ plot, one has to draw a line through that point, which is perpendicular to the X axis. The intersection of this line with the x axis (corresponding to $M = 0$) gives the value of H/M. We then draw a new Y axis perpendicular to the X axis. This axis represents the locus of all points with $H/M = 0$. Whenever an Arrott-plot trajectory corresponding to a given temperature t intersects the Y axis at a point $Y > 0$, a solution with $M \neq 0$ and $H = 0$ exists. For fixed finite Δ_F (or Δ_A) the rotated M^2 axis will start cutting the isotherms (Fig. 3) only for angles above some threshold. Since the low-temperature isotherms have a convex shape, the axis will cut isotherms twice, and only the upper intercept will be a legitimate solution for M^2. The new Arrott plots (M^2 vs H/M) for $v_4 > 0$ are displayed in Figs. 7(a) and 7(b) for the cases of a random field and a random anisotropy, respectively. We thus expect *first-order* transitions directly into the ferromagnetic phase at sufficiently large v_4. Except for this difference and changes in slope and curvature of the phase boundaries, the v_4-Δ-T phase diagrams are expected to be similar to those shown in Fig. 4.

In the case of the hexagonal asymmetry (1.9), we obtain in the large-N limit

$$r_T = H/M + v_6 M^4 , \tag{2.4}$$

so that the mapping of the Arrott plots involves both a rotation and a curvature [$M^2 \to (M^2)^2$]. When $\Delta_F = \Delta_A = 0$ the large-N analysis shows a clear difference between the phase diagrams for the cases $d < 3$ and $d \geq 3$. For $d \geq 3$ a small v_6 does not stabilize a ferromagnetic phase for $T > T_c$, where T_c is the critical temperature of the isotropic system. This is related to the fact that the dimension of the operator (1.9) in the large-N limit is equal to its naive dimensions and is an irrelevant operator above three

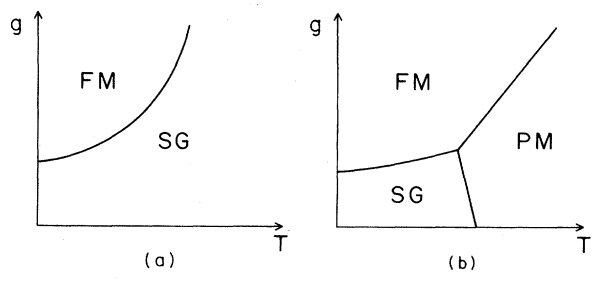

FIG. 5. (a) A g-T phase diagram for the random-field case. (b) A g-T phase diagram for the random-anisotropy case.

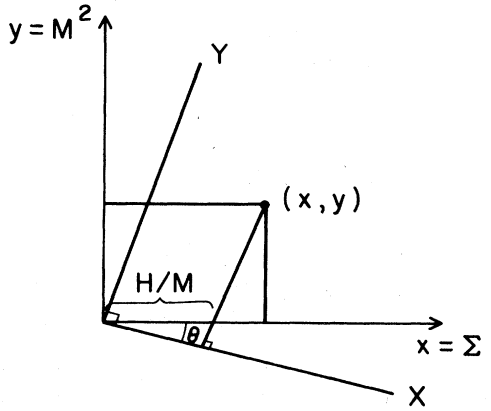

FIG. 6. Determination of the Arrott plot in the presence of a cubic asymmetry from the Arrott plots of the isotropic case.

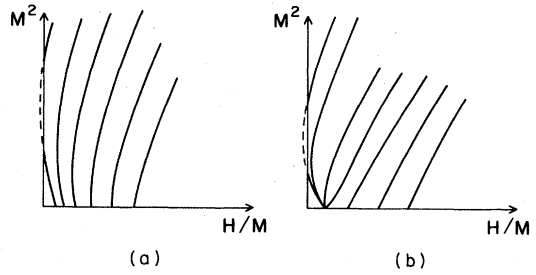

FIG. 7. (a) Modified Arrott plots for the random-field case in the presence of a cubic anisotropy. (b) Same as (a) for the random-anisotropy model.

dimensions. For finite N, there is a dimensionality $d_c(N)$ below which the operator starts to become relevant (and its corresponding eigenvalue changes sign). When $d < d_c(N)$ the situation is similar to the case of a cubic anisotropy below four dimensions.

When Δ_F or Δ_A are nonzero, one again has to distinguish the case $d > d_c(N)$ and $d < d_c(N)$. In the first case, as one increases v_6 a first-order transition into a ferromagnetic phase occurs only for $T < T_c(\Delta)$ with $T_c(\Delta) \leqq T_c$. This means that for $T = T_c$ and small v_6, no transition takes place. For $d < d_c(N)$ the phase diagram is similar to the case of a cubic anisotropy. For large N, even for $d=3$ we find no transition at $T = T_c$.

III. LOW-TEMPERATURE DOMAIN STABILITY

In addition to the argument involving Eq. (1.6), Imry and Ma[1] also used the following domain argument: At low temperature, the fully ordered ground state will break into finite domains of linear size L if the gained bulk energy $E_B \sim (\Delta_F L^d)^{1/2}$ (due to ordering along the local average random field) is larger than the energy cost of the domain surface E_s. For isotropic spin systems, E_s is of order JL^{d-2} (where J is the nearest-neighbor exchange energy) and domains will occur for $d < 4$. The typical size of the domains is estimated by minimizing $(E_s - E_B)$:

$$L_0 \sim \left[\frac{J}{\Delta_F^{1/2}} \right]^{2/(4-d)} . \tag{3.1}$$

For Ising systems, E_s is of order JL^{d-1}, and domains are preferred only for $d < 2$.

In what follows, we shall show that any anisotropy which breaks the rotational invariance causes a crossover from $E_s \sim L^{d-2}$ to $E_s \sim L^{d-1}$, and thus to ferromagnetic long-range order at $2 < d < 4$. The aim of the following discussion is to estimate the threshold anisotropy (g, v_4, v_6, etc.) above which this happens.

Consider first the uniaxially anisotropic case, Eq. (1.10). If the angle between $\mathbf{S}(x)$ and the S^1 axis is θ and the domain "wall" extends (along the x axis) from $x=0$ to $x = x_0$, then the optimum function $\theta(x)$ should minimize the wall energy (per unit area). The incremental wall energy with respect to a configuration with $\theta(x) \equiv 0$, is given by

$$E_w\{\theta(x)\} = J \int_0^{x_0} dx \left[\frac{d\theta}{dx} \right]^2 + g \int_0^{x_0} dx \left[\frac{N-1}{N} + \frac{1}{N} \sin^2\theta - \frac{N-1}{N} \cos^2\theta \right], \tag{3.2}$$

subject to $\theta(0)=0$, $\theta(x_0)=\pi$. Taking the functional derivative

$$\frac{\delta E_w}{\delta \theta(x)} = -2J \frac{d^2\theta}{dx^2} + g \sin(2\theta) = 0 , \tag{3.3}$$

the solution becomes

$$\theta(x) = \frac{\pi}{x_0} x - \frac{g x_0^2}{8J\pi^2} \sin \left[\frac{2\pi x}{x_0} \right] + O(g^2) , \tag{3.4}$$

hence,

$$E_w = J\pi^2/x_0 + \tfrac{1}{2} g x_0 + O(g^2) \tag{3.5}$$

and E_w is minimal when

$$x_0 = \left[\frac{2J\pi^2}{g} \right]^{1/2} \tag{3.6}$$

with

$$E_w = \pi (2Jg)^{1/2} . \tag{3.7}$$

Equation (3.5) might be expected on an heuristic basis: The first term, representing the exchange energy, results from assuming that the angle between two neighboring spins is of order (π/x_0). The second term implies that each spin contributes an anisotropy energy of order g. Indeed, we show below that this behavior is quite general.

If the domain size L is much larger than x_0, then the wall energy is $E_s = E_w L^{d-1}$, and we expect the Ising-like behavior. On the other hand, the above calculation should not be used when $L \ll x_0$. In this limit, we should use Eq. (3.4) with L instead of x_0, and we are back at the isotropic situation, yielding (3.1). The crossover between the two will occur when $x_0 \sim L_0$, where L_0 was defined in Eq. (3.1), i.e.,

$$\frac{g}{J} \sim \left[\frac{\Delta_F}{J^2} \right]^{2/(4-d)} . \tag{3.8}$$

This equation represents the border line between the FM and the SG phases on the Δ_F-g plane, Fig. 4. If we start at zero temperature and $2 < d < 4$ with $g=0$, then we have no long-range order due to the existence of domains. Increasing g beyond the value (3.8) will recover FM long-range order. The nature of the transition at this critical value of g remains to be studied.

The argument presented above should equally apply to the case of random uniaxial anisotropies. At low temperature, these systems are also expected to break into ordered domains, within which there is full ordering along the local average anisotropy axis. Since the magnetization is practically saturated, all one needs to do is replace Δ_F in the above results by Δ_A (or w^2).

The result (3.8) also applies to the higher-order anisotropies, Eqs. (1.8), (1.9), etc. For example, consider the cubic case (1.8). For $v_4>0$, domains are ordered along cubic axes. Consider now two neighboring domains ordered along perpendicular axes. If the angle between $\mathbf{S}(x)$ and one of these axes is θ, then (2.2) will be replaced by

$$E_w\{\theta(x)\}=J\int_0^{x_0}dx\left[\frac{d\theta}{dx}\right]^2 +v_4\int_0^{x_0}dx(1-\cos^4\theta-\sin^4\theta)\ , \tag{3.9}$$

subject to $\theta(0)=0$, $\theta(x_0)=\pi/2$. One can then repeat all the other steps as described above and find a transition from a domain state to a FM phase at

$$\frac{v_4}{J}\sim\left[\frac{\Delta_F}{J^2}\right]^{2/(4-d)}\ . \tag{3.10}$$

Similar results apply to v_6, etc.

The above results find support in the renormalization-group equations near zero temperature.[16,17] In this limit, the scaling behavior is given simply by the naive dimension of the different operators. If the lengths are scaled by a factor b, then

$$T\to b^{2-d}T\ , \tag{3.11}$$

$$\frac{\Delta_F}{T^2}\to b^d\frac{\Delta_F}{T^2}\ , \tag{3.12}$$

$$\frac{g}{T}\to b^d\frac{g}{T}\ , \tag{3.13}$$

$$\frac{v_4}{T}\to b^d\frac{v_4}{T}\ , \tag{3.14}$$

etc., and therefore

$$g\to b^2 g\ , \tag{3.15}$$

$$v_4\to b^2 v_4\ , \tag{3.16}$$

$$\Delta_F\to b^{4-d}\Delta_F\ . \tag{3.17}$$

Iterating (3.17) until $\Delta_F\sim 1$ and substituting the corresponding value of b into (3.15) or (3.16), yields (3.8) or (3.10). As we shall see in the next section, these are special cases of a general scaling approach.

IV. SCALING

Near the isotropic ordered transition point, the equation of state can be written in the scaling form

$$\frac{H}{M^\delta}=\tilde f\left[\frac{t}{M^{1/\beta}},\frac{\Delta_F}{|t|^{\phi_F}},\frac{\Delta_A}{|t|^{\phi_A}},\frac{g}{|t|^{\phi_g}},\frac{v_4}{|t|^{\phi_4}},\frac{v_6}{|t|^{\phi_6}},\dots\right]\ , \tag{4.1}$$

where $t=(T-T_c)/T_c$ (T_c is the ordering transition of the pure isotropic system) and where the various crossover exponents ϕ_i are directly related to the scaling of the appropriate fields near the isotropic fixed point. For example, $\phi_g=\lambda_g\nu$, where $g\to b^{\lambda_g}g$ and ν is the correlation-length exponent.[18] The exponent ϕ_F is known to be exactly equal to the susceptibility exponent γ.[19] Similarly, the exponent ϕ_A has been exactly related to ϕ_g,[12]

$$\phi_A=2\phi_g-d\nu\ . \tag{4.2}$$

All the exponents in Eq. (4.1) are known within ϵ expansions in $4-\epsilon$ and in $2+\tilde\epsilon$ dimensions and within the $1/N$ expansion. We list these expansions in Table I.

Typically, we shall be concerned with either Δ_F or Δ_A, and with one of g, v_4, v_6, etc. Consider, for example, the case in which Δ_A and v_4 are nonzero. Thus,

$$\frac{H}{M^\delta}=\tilde f\left[\frac{t}{M^{1/\beta}},\frac{\Delta_A}{|t|^{\phi_A}},\frac{v_4}{|t|^{\phi_4}}\right]\ . \tag{4.3}$$

When both Δ_A and v_4 are zero, Eq. (4.3) has a nonzero solution for $M\neq 0$ in the limit $H\to 0$ when $t<0$. This solution no longer exists for $\Delta_A>0$ and small v_4 but is expected to reappear at some (Δ_A-dependent) finite value of v_4. Within the scaling approach, this implies that the function $f(x,y,z)$ is singular along some line in the y-z plane. Since we expect this line to go through the origin, its general form near the origin is[20] $z\sim y^{\theta_{4A}}$, or

$$\frac{v_4}{|t|^{\phi_4}}\sim\left[\frac{\Delta_A}{|t|^{\phi_A}}\right]^{\theta_{4A}}\ . \tag{4.4}$$

In the absence of Δ_A, v_4 tends to increase T_c (see below). Thus, one might hope to find a transition at sufficiently small Δ_A even at $t=0$. In this case, $|t|$ should drop out of (4.4), and we predict that

$$\phi_{4A}=\phi_4/\phi_A \tag{4.5}$$

and

$$v_4\sim\Delta_A^{\theta_{4A}}\ . \tag{4.6}$$

Similarly, we predict $\theta_{gA}=\phi_g/\phi_A$, $\theta_{6A}=\phi_6/\phi_A$ (whenever it is positive), $\theta_{4F}=\phi_4/\phi_F$, etc., for the other self-explanatory cases. With continuity, it is reasonable to expect a behavior like (4.6) at other temperatures as well. Indeed, our zero-temperature result (3.8) confirms this expectation, with $\theta_{gF}=2/(4-d)=\phi_g/\phi_F=\lambda_g/\lambda_F$ [see Eqs. (3.15) and (3.17)]. At $T=0$, it turns out that *all* the exponents θ_{ij} have the same value, i.e., $2/(4-d)$. Our general expectations for the exponents θ_{ij} can be directly read from Table I.

V. HAMILTONIAN AND EQUATION OF STATE FOR $N\to\infty$

As in all the field-theoretical calculations, we start with an isotropic Ginzburg-Landau-Wilson Hamiltonian,[18]

TABLE I. Values of crossover exponents for the different operators. The corresponding eigenvalues are given by $\lambda_i=\phi_i/\nu$.

Exponent	$d=4-\epsilon$[a]	$d=2+\tilde{\epsilon}$[b]	Large N[c] ($d<4$)[d]	$T=0$
$\phi_F=\gamma$	$1+\frac{N+2}{2(N+8)}\epsilon+\frac{(N+2)(N^2+22N+52)}{4(N+8)^3}\epsilon^2+\cdots$	$\frac{2}{\tilde{\epsilon}}\left[1-\frac{3\tilde{\epsilon}}{2(N-2)}+\frac{2\tilde{\epsilon}^2}{(N-2)^2}+\cdots\right]$	$\frac{2}{d-2}\left[1-\frac{6S_d}{N}+\cdots\right]$	$\frac{4-d}{2-d}$
ϕ_A	$\frac{N+4}{2(N+8)}\epsilon+\frac{N^3+16N^2+20N-112}{4(N+8)^3}\epsilon^2+\cdots$	$\frac{2}{\tilde{\epsilon}}\left[1-\frac{N+4}{2(N-2)}\tilde{\epsilon}+\frac{N+3}{(N-2)^2}\tilde{\epsilon}^2+\cdots\right]$	$\frac{4-d}{d-2}\left[1-8\frac{5-d}{4d}\frac{S_d}{N}+\cdots\right]$	$\frac{4-d}{2-d}$
ϕ_g	$1+\frac{N}{2(N+8)}\epsilon+\frac{N^2+24N^2+68N}{4(N+8)^3}\epsilon^2+\cdots$	$\frac{2}{\tilde{\epsilon}}\left[1-\frac{2\tilde{\epsilon}}{N-2}+\frac{3\tilde{\epsilon}^2}{(N-2)^2}+\cdots\right]$	$\frac{2}{d-2}\left[1-\frac{8S_d}{N}+\cdots\right]$	$\frac{2}{2-d}$
ϕ_4	$\frac{N-4}{2(N+8)}\epsilon+\frac{N^316N^2+4N+240}{4(N+8)^3}\epsilon^2+\cdots$	$\frac{2}{\tilde{\epsilon}}\left[1-\frac{N+8}{2(N-2)}\tilde{\epsilon}+\frac{N+7}{(N-2)^2}\tilde{\epsilon}^2+\cdots\right]$	$\frac{4-d}{d-2}\left[1-8\frac{7-d}{4-d}\frac{S_d}{N}+\cdots\right]$	$\frac{2}{2-d}$
ϕ_6	$-1+\frac{N-16}{2(N+8)}\epsilon+\frac{N^3+8N^2+116N+2368}{4(N+8)^3}\epsilon^2+\cdots$	$\frac{2}{\tilde{\epsilon}}\left[1-\frac{N+8}{N-2}\tilde{\epsilon}+\frac{2N+15}{(N-2)^2}\tilde{\epsilon}^2+\cdots\right]$	$-2\frac{d-3}{d-2}+\cdots$	$\frac{2}{2-d}$
ν	$\frac{1}{2}+\frac{N+2}{4(N+8)}\epsilon+\frac{(N+2)(N^2+23N+60)}{8(N+8)^3}\epsilon^2+\cdots$	$\frac{1}{\tilde{\epsilon}}\left[1-\frac{1}{N-2}\tilde{\epsilon}-\frac{N-4}{2(N-2)^2}\tilde{\epsilon}^2+\cdots\right]$	$\frac{1}{d-2}\left[1-\frac{8(d-1)}{d}\frac{S_d}{N}+\cdots\right]$	$\frac{1}{2-d}$

[a]References 18, 30, and 31.

[b]References 16, 32, and 33.

[c]Reference 30.

[d]$S_d=\frac{\sin[\pi(\frac{1}{2}d-1)]\Gamma(d-1)}{2\pi\Gamma(d/2)^2}$, $S_{4-\epsilon}=\frac{\epsilon}{2}-\frac{\epsilon^2}{4}+O(\epsilon^3)$, $S_{2+\tilde{\epsilon}}=\frac{\tilde{\epsilon}^2}{4}+O(\tilde{\epsilon}^3)$, $S_3=\frac{2}{\pi^2}$.

$$\mathscr{H}_0=-\int d^dx\{\tfrac{1}{2}[(\nabla\mathbf{S})^2+m_0^2|\mathbf{S}|^2]+(u/4!N)|\mathbf{S}|^4\}\ , \tag{5.1}$$

where $\mathbf{S}(x)$ is now a continuous spin at the continuous d-dimensional space coordinate x, and where m_0^2 is linear in T, $m_0^2\propto(T-T_c)$. The anisotropy terms, e.g., (1.8)—(1.10) are then added with $\sum_x$ being replaced by $\int d^dx$. To treat the random terms (1.1) and (1.3), one replicates the system n times, averages over the random variables, and takes the limit $n\to 0$ at the end.[12,18] The resulting replicated Hamiltonian has the form[8,12,18]

$$\mathscr{H}=\int d^dx\left\{\sum_{\alpha=1}^{n}\left[\tfrac{1}{2}[|\nabla\mathbf{S}_\alpha(x)|^2+m_0^2|\mathbf{S}_\alpha|^2]+\frac{u}{4!N}|\mathbf{S}_\alpha|^4+g\left[\frac{1}{N}\sum_{i=2}^{N}(S_\alpha^i)^2+\frac{1-N}{N}(S_\alpha^1)^2\right]\right.\right.$$
$$\left.\left.-\frac{v_4}{4N}\sum_i(S_\alpha^i)^4-\frac{v_6}{6N^6}\sum_i(S_\alpha^i)^6\right]-\Delta_F\sum_{i=1}^{N}\sum_{\alpha,\beta=1}^{n}S_\alpha^iS_\beta^i-\frac{\Delta_A}{4!N}\sum_{i,j=1}^{N}\sum_{\alpha,\beta=1}^{n}S_\alpha^iS_\beta^iS_\alpha^jS_\beta^j\right\}, \tag{5.2}$$

where α,β are the replica indices. We have scaled u, Δ_A, and v_4 like N^{-1}, in order to achieve an appropriate large-N limit, whereas v_6 is scaled like $1/N^2$. The choice of the cubic term as being of order N^{-1} is appropriate[21] for the case $v_4>0$, and this will be the only case we shall treat here.

We note that, in general, $\mathscr{H}$ will contain additional quartic terms, e.g., those representing random exchange (i.e., $S_\alpha^iS_\alpha^iS_\beta^jS_\beta^j$, see Ref. 12). These are highly irrelevant for large N, and therefore are ignored here (as they were in Refs. 2 and 8).

In order to derive the equation of state, we apply a magnetic field along an easy axis, say $i=1$:

$$-H\int d^dx\sum_{\alpha=1}^{n}S_\alpha^1(x)\ . \tag{5.3}$$

Shifting the longitudinal component to allow for a nonzero magnetization, we define

$$L_\alpha(x)=S_\alpha^1(x)-M \tag{5.4}$$

and demand that

$$\langle L_\alpha(x)\rangle=0\ . \tag{5.5}$$

To represent this equation graphically in the large-N limit, we use the notation of Ref. 8. The graphs corresponding to the vertices g, Δ_F, Δ_A, u, v_4, and v_6 are represented in Fig. 8. The graphs corresponding to the Edwards-Anderson order parameter

$$q=\sum_i\langle S_\alpha^i(x)S_\beta^i(x)\rangle\quad(\alpha\neq\beta)$$

in the large-N limit are depicted in Fig. 9. The graphs representing Eq. (5.5) are depicted in Fig. 10 and those contributing to the equation for the transverse mass Σ, in Fig. 11. Defining $G_T(k)$ as the transverse two-point correlation function,

$$G_T(k)=\lim_{n\to 0}\frac{1}{n}\sum_{\alpha=1}^{n}\int d^dx\langle S_\alpha^i(x)S_\alpha^i(0)\rangle e^{ikx},\quad i\geq 2\ , \tag{5.6}$$

this function is given in the large-N limit by

$$G_T^{-1}(k)=k^2+\Sigma\ . \tag{5.7}$$

We then find that Eq. (5.5) corresponds to

$$\frac{H}{M}=m_0^2-g+\tfrac{1}{6}(u-\Delta_A)\int_p G_T(p)+\frac{u}{6N}q-\frac{v_4}{N}M^2-\frac{v_6}{N^2}M^4\ , \tag{5.8}$$

and the equation for Σ is

$$\Sigma=m_0^2+\tfrac{1}{6}(u-\Delta_A)\int_p G_T(p)+\frac{u}{6N}q\ , \tag{5.9}$$

where in (5.8) and (5.9)

$$\int_p\equiv(2\pi)^{-d}\int d^dp\ .$$

Combining these two equations with the equation for q (Fig. 9)

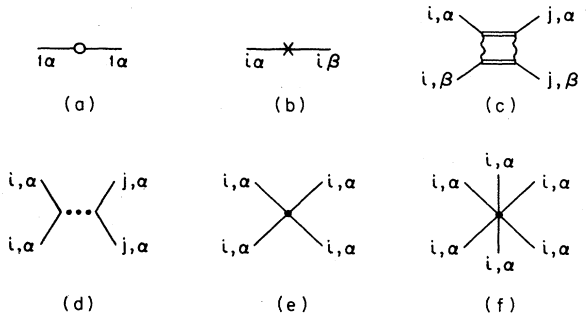

FIG. 8. Graphical notation for the different vertices (a) g, (b) Δ_F, (c) Δ_A, (d) u, (e) v_4, and (f) v_6.

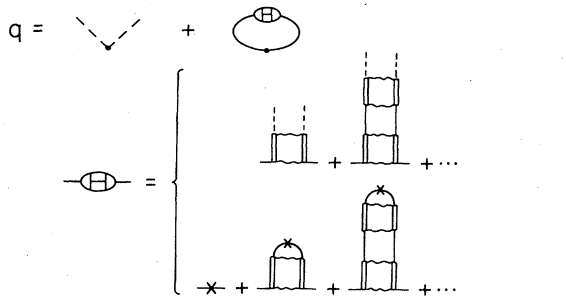

FIG. 9. Diagrams contributing to q, the Edwards-Anderson order parameter. The dashed line stands for M, where M denotes the magnetization. The dots stand for an infinite set of diagrams of the ladder type.

$$q=\frac{M^2+N\Delta_F\int_p G_T(p)^2}{1-\frac{1}{6}\Delta_A\int_p G_T(p)^2}\ , \tag{5.10}$$

we find

$$\Sigma=\frac{H}{M}+g+\frac{v_4}{N}M^2+\frac{v_6}{N^2}M^4\ , \tag{5.11}$$

$$\Sigma=m_0^2+\tfrac{1}{6}(u-\Delta_A)\int_p\frac{1}{p^2+\Sigma}+\frac{u}{6N}\left[M^2+N\Delta_F\int_p\frac{1}{(p^2+\Sigma)^2}\right]\Big/\left[1-\tfrac{1}{6}\Delta_A\int_p\frac{1}{(p^2+\Sigma)^2}\right]\ . \tag{5.12}$$

Equation (5.12) for Σ is the same as that found for H/M in the isotopic case.[8] The only difference is that Σ, as given by Eq. (5.11), replaces H/M. This yields all the rules concerning the shifting and rotating of the Arrott plots, as described in Sec. II.

For $2<d<4$, Eq. (5.12) may be written as[8]

$$\Sigma=m^2-\tfrac{1}{6}(u-\Delta_A)f_1(d)\Sigma^{1-\epsilon/2}+\frac{u}{6N}[M^2+N\Delta_F f_2(d)\Sigma^{-\epsilon/2}]\Big/\left[1-\frac{\Delta_A}{6}f_2(d)\Sigma^{-\epsilon/2}\right], \tag{5.13}$$

where $\epsilon=4-d$, m^2 is a renormalized mass,

$$m^2=m_0^2+\tfrac{1}{6}(u-\Delta_A)\int_p^{\Lambda}\frac{1}{p^2}\ , \tag{5.14}$$

$$f_1(d)=\int_p\frac{1}{p^2(p^2+1)},\quad f_2(d)=\int_p\frac{1}{(p^2+1)^2}\ . \tag{5.15}$$

It can easily be shown that the equations of state (5.13) may be expressed in the scaling form (4.1). Replacing M^2/N by $M^2=O(1)$, and defining

$$t=\frac{6}{u}m^2 \tag{5.16}$$

and replacing $(u-\Delta)/u\sim 1$ near the isotropic fixed point we find

$$\frac{H}{M^\delta}+\frac{g}{M^{\sigma_g}}+\frac{v_2}{M^{\sigma_4}}+\frac{v_6}{M^{\sigma_6}}=f_1^{-\gamma}\left\{\frac{t}{M^{1/\beta}}+\left[1-\frac{f_2\Delta_A}{6M^{\sigma_A}}\left[\frac{H}{M^\delta}+\frac{g}{M^{\sigma_g}}+\frac{v_4}{M^{\sigma_4}}+\frac{v_6}{M^{\sigma_6}}\right]^{-1/\gamma_\Delta}\right]^{-1}\right.$$
$$\left.\times\left[1+\frac{f_2\Delta_F}{M^{\sigma_F}}\left[\frac{H}{M^\delta}+\frac{g}{M^{\sigma_6}}+\frac{v_4}{M^{\sigma_4}}+\frac{v_6}{M^{\sigma_6}}\right]^{-1/\gamma_\Delta}\right]\right\}^{\gamma} \tag{5.17}$$

with $d=4-\epsilon$,

$$\beta=\tfrac{1}{2},\quad \delta=3+\frac{2\epsilon}{2-\epsilon}\ , \tag{5.18}$$

$$\gamma=\frac{2}{2-\epsilon},\quad \gamma_\Delta=\frac{2}{\epsilon}\ , \tag{5.19}$$

$$\sigma_g=2+\frac{2\epsilon}{2-\epsilon},\quad \sigma_4=\frac{2\epsilon}{2-\epsilon},\quad \sigma_6=-2+\frac{2\epsilon}{2-\epsilon}\ , \tag{5.20}$$

$$\sigma_A=\frac{2\epsilon}{2-\epsilon},\quad \sigma_F=\frac{4}{2-\epsilon}\ . \tag{5.21}$$

The exponents σ_i for $i=g,4,6,A,F$ are related to ϕ_i by $\sigma_i=\phi_i/\beta$. Indeed the values given by Eqs. (5.20) and (5.21) agree with the values of ϕ_i given in Table I in the large-N limit.

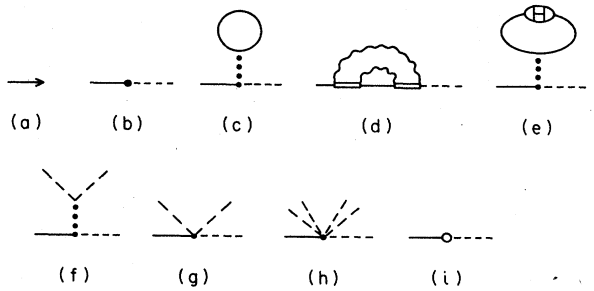

FIG. 10. Diagrams representing Eq. (5.5). The dot stands for m_0^2. The arrow stands for an applied field H.

VI. EXAMPLE: THE CUBIC CASE WITH RA

To demonstrate how the equation of state (5.13) yields the general results described in Sec. II, we give here a detailed analysis of the most disputed case of a cubic system with random uniaxial anisotropies, in which we find a first-order transition. For brevity, we use $v_4=v$ and $\Delta_A=\Delta$. For $v=0$ the large-N theory in dimensions $2<d<4$ possesses two different phases: a paramagnetic phase and a spin-glass phase depending upon $t>t_c$ or $t<t_c$, where

$$t_c=f_1\Sigma_c^{1-\epsilon/2},\quad \Sigma_c=(\tfrac{1}{6}f_2\Delta)^{1/\epsilon}\ . \tag{6.1}$$

When $v>0$ the system can have a ferromagnetic phase, as can be shown by an investigation of the equation of

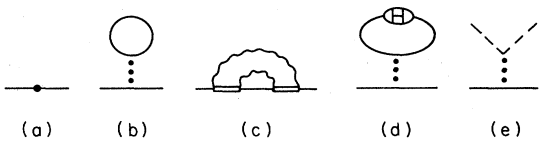

FIG. 11. Equation for the self-energy Σ (the transverse mass). The dot stands for m_0^2.

state and the free energy of the system. We start by considering the equation of state; the discussion of the free energy follows.

Consider first the case $t=0$. We look for a solution of Eq. (5.17) with $M\neq 0$ for $H=0$. We obtain

$$f_1(v/M^{\sigma_4})^{1/\gamma}=\left[1-\tfrac{1}{6}f_2\frac{\Delta}{M^{\sigma_A}}\left[\frac{v}{M^{\sigma_4}}\right]^{-1/\gamma_\Delta}\right]^{-1} \tag{6.2}$$

and, substituting for the exponents from Eq. (5.18) through (5.20), we find

$$(M^\epsilon)^2-f_1 v^{(2-\epsilon)/2}M^\epsilon+\tfrac{1}{6}\Delta f_1 f_2 v^{1-\epsilon}=0\ , \tag{6.3}$$

whose solution is

$$M^\epsilon=\tfrac{1}{2}f_1\left[v^{(2-\epsilon)/2}\pm\left[v^{2-\epsilon}-\frac{2}{3}\frac{f_2}{f_1}\Delta v^{1-\epsilon}\right]^{1/2}\right]\ . \tag{6.4}$$

The positive sign before the square root gives the stable solution in the case $\Delta=0$, so it is expected to be the stable solution for $\Delta>0$. We see that a real solution ceases to exist whenever the argument of the square root becomes negative, i.e., for

$$v<\frac{2}{3}\frac{f_2}{f_1}\Delta \tag{6.5}$$

in any dimension. This is consistent with the phase boundary at $t=0$ given by Eq. (4.6) with $\theta=1$. Actually, by considering the free energy, it will turn out that the tion with $M\neq 0$ will become unstable even before (for higher values of v), but this only means that the coefficient of Δ on the right-hand side of Eq. (6.5) has to be modified while the scaling exponent θ remains correct. We also see that the transition is first order since M has a finite discontinuity at the phase boundary. In the general case $t\neq 0$ we consider only the physically interesting case $\epsilon=1$. In that case we obtain the following equation for the magnetization for $H=0$:

$$M^3-f_1\sqrt{v}M^2+(t+\tfrac{1}{6}f_1f_2\Delta)M-\tfrac{1}{6}f_2\frac{t\Delta}{\sqrt{v}}=0\ . \tag{6.6}$$

It is possible to investigate this cubic equation and we find that the locus of points for which the solution ceases to be real is given by the equation

$$\begin{aligned}(3t+\tfrac{1}{2}f_1f_2\Delta-f_1^2v)^3+\tfrac{1}{4}[&-2f_1^3v\sqrt{v}\\&+9f_1\sqrt{v}\,(t+\tfrac{1}{6}f_1f_2\Delta)\\&-9f_2t\Delta/2\sqrt{v}\,]^2=0\ .\end{aligned} \tag{6.7}$$

At the phase boundary, the magnetization is given by

$$M=\tfrac{1}{3}f_1\sqrt{v}+\tfrac{1}{3}(f_1^2v-3t-\tfrac{1}{2}f_1f_2\Delta)^{1/2}\ . \tag{6.8}$$

For $\Delta=0$, Eq. (6.7) represents a straight line $t=f_1^2v/4$ in the v-t plane. For $\Delta>0$ and $t\to-\infty$, it is consistent with $v\propto\Delta^2/|t|$. As we argued in Sec. III, at $T=0$, there is a phase transition for nonzero v whenever $\Delta\neq 0$, and the phase boundary is given by $v\propto\Delta^2$ in three dimensions and more generally by $v\propto\Delta^{2/(4-d)}$ in d dimensions.

Whenever there is no solution with $M\neq 0$, or the $M\neq 0$ solution is unstable, the solution of the equation of state coincides with that of the $v=0$ case, as follows from Eqs. (5.11) and (5.12) with g and v_6 set to zero. In particular, when $M=0$, the phase boundary between the spin glass $q\neq 0$ and the paramagnetic phase does not depend on v.

A schematic phase diagram for large N is depicted in Fig. 12, representing the v-T plane for fixed $\Delta>0$. Figure 13 represents the phase diagram in the v-T plane for fixed $\Delta\neq 0$. These diagrams describe the $N=\infty$ case. For finite N, we might expect the slope and curvature of the phase boundary to change. Generic phase diagrams have already been displayed in Sec. II but here we display them to show the particular characteristics of the $N=\infty$ case with cubic symmetry breaking.

We now turn to check the free energy. For $v>0$, this is obtained using a functional integral technique (Appendix A) and we find

$$\begin{aligned}\frac{F}{N}=&-vM^4+\tfrac{1}{2}\Sigma M^2-\tfrac{1}{24}\Delta q^2\\&-\frac{3}{2(u-\Delta)}\left[\Sigma-\frac{\Delta}{6}q-m_0^2\right]^2\\&+\tfrac{1}{2}\int_p\ln(p^2+\Sigma)-\frac{\Delta q}{12}\int_p\frac{1}{p^2+\Sigma}\ ,\end{aligned} \tag{6.9}$$

where we have again rescaled M^2 and q to be of order 1. In this equation, Σ is a function of M^2 and q is determined from the equation

$$\frac{\partial F}{\partial\Sigma}=0\ . \tag{6.10}$$

The other two equations $\partial F/\partial q=0$ and $\partial F/\partial M=0$ determine the equation of state as can be readily verified. Using Eqs. (5.14) and (5.16) with $g=0$ and carrying out the integrals, Eq. (6.9) can be written as

$$\begin{aligned}F=&-\tfrac{1}{4}vM^4+\tfrac{1}{2}\Sigma M^2-\tfrac{1}{24}\Delta q^2\\&-\frac{3}{2(u-\Delta)}\left[\Sigma-\frac{\Delta}{6}q-\frac{u}{6}t\right]^2\\&-\tfrac{1}{2}f_1\Sigma^{d/2}+\tfrac{1}{12}\Delta q f_1\Sigma^{(d-2)/2}+\tilde{F}(t)\ ,\end{aligned} \tag{6.11}$$

where $\tilde{F}(t)$ is a linear function of t, which is cutoff dependent. We have investigated Eq. (6.11) for the case $t=0$

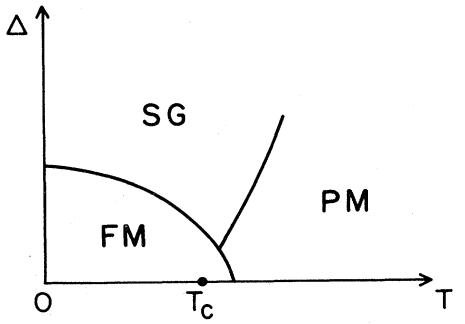

FIG. 12. A Δ-T phase diagram for the case of cubic anisotropy in the large-N limit.

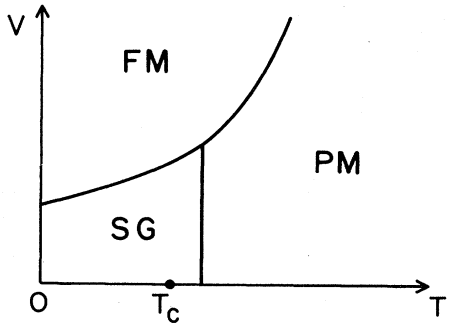

FIG. 13. A v-T phase diagram for the case of random anisotropy in the large-N limit.

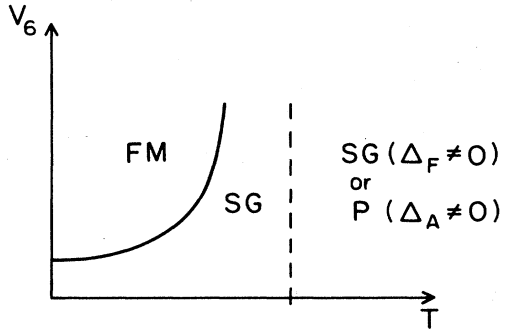

FIG. 14. A v_6-T phase diagram for $d=3$. In the case of random anisotropy, the dashed line separates the spin-glass phase from the paramagnetic phase. This lines does not exist for the random-field case.

and $d=3$, and considered two possible solutions: a spin-glass solution and a ferromagnetic solution. In Appendix B we show that whenever $\Delta \ll v$ the ferromagnetic solution has lower energy. At the point $\Delta=(3f_1/2f_2)v$ where the investigation of the equation of state predicts that the ferromagnetic solution starts becoming complex we find that the spin-glass solution has lower energy, so that the phase transition actually occurs for a higher value of v.

VII. OTHER CASES OF INTEREST

In this section, we outline the treatment of the other cases discussed in Secs. II and Sec. V. In the random-field case with cubic anisotropy, the $\epsilon=1$, large-N equation of state reads, when $M\neq 0$ for $H=0$ [compare with Eq. (5.17); we have absorbed a factor f_2 in Δ_F],

$$\frac{v}{M^2}=f_1^{-2}\left[\frac{t}{M^2}+1+\frac{\Delta_F}{M^4}\left[\frac{v}{M^2}\right]^{-1/2}\right]^2 \tag{7.1}$$

or

$$M^3-f_1\sqrt{v}M^2+tM+\frac{\Delta_F}{\sqrt{v}}=0\ . \tag{7.2}$$

The locus of points for which the solution ceases to be real is given by

$$(3t-f_1^2v)^3+\tfrac{1}{4}[-2f_1^3v\sqrt{v}+9f_1\sqrt{v}t+27\Delta_F/\sqrt{v}\,]^2=0\ . \tag{7.3}$$

For $t=0$ this yields

$$\Delta_F=\tfrac{4}{27}f_1^3v^2\ , \tag{7.4}$$

which is consistent with $\theta_{4F}=\frac{1}{2}$ for large N (compare with ϕ_4/ϕ_F in Table I). The situation for a quadratic symmetry breaking is very similar, the only qualitative difference is, as indicated in Sec. II, that the transition into the ferromagnetic phase is second order both from the paramagnetic and from the spin-glass phases. The exponents in the large-N limit are those of the mean-field spherical model, as was noted previously[22] for a transition from $N\to\infty$ to a finite number of soft components. But for finite N, the transition should be that of the pure Ising model for a transition from the paramagnetic phase to the ferromagnetic one (for $\Delta_A\neq 0$) and that of an Ising model in a random field for the transition from the spin-glass to the ferromagnetic phase (for $\Delta_F\neq 0$ or $\Delta_A\neq 0$).

For the case of sixfold anisotropy (1.9), we can again investigate the equation of state assuming $M\neq 0$ for $H=0$. When $\Delta_F\neq 0$ we obtain for $d=3$:

$$[1-f_1(v_6)^{1/2}]M^4+tM^2+\frac{\Delta_F}{(v_6)^{1/2}}=0\ . \tag{7.5}$$

The solution with M real ceases to exist when

$$\frac{4\Delta_F[1-f_1(v_6)^{1/2}]}{(v_6)^{1/2}}>t^2 \tag{7.6}$$

and thus the phase boundary is given approximately by

$$v_6\sim\frac{16\Delta_F^2}{t^4}\ . \tag{7.7}$$

Note that the analysis is valid only for small v_6 ($v_6<1$), otherwise we go out of the domain of stability of the model, and higher-order operators have to be added. Equation (7.7) implies that the phase boundary in the v_6-T plane diverges for $t\to 0$ from below. An investigation of the free energy is necessary to determine whether the transition does not actually occur for lower T. A v_6-T phase diagram for $N=\infty$ and $d=3$ is depicted in Fig. 14.

Similarly for the random-anisotropy case, an investigation of the equation of state reveals that the phase boundary is given approximately for $v_6<1$ by

$$v_6\sim\frac{\Delta_A^2\,|\,t\,|^2}{(\,|\,t\,|-\Delta)^4} \tag{7.8}$$

for $t<0$. Again the accurate location of the transition can be obtained from the behavior of the free energy.

VIII. DISCUSSION

As discussed in Refs. 3 and 13, many real systems have *random uniaxial anisotropies* (or equivalent random terms), and long-range order is stabilized in them only because they also have *uniform anisotropies.* At finite values of these (cubic or higher-order) uniform anisotropies, we predict the typical phase diagrams of Figs. 4(b) or 5(b). In some cases, a spin-glass phase will precede (or replace) the ferromagnetic phase, and in others, the transition will become first order. In most real systems Δ_A is small compared to the relevant uniform anisotropy parameter (e.g., $v_4^{1/\theta_{4A}}$), so that the first-order effect may be small (i.e., a small discontinuity very close to the continuous transition). It would be very interesting to find real systems in which Δ_A is sufficiently strong to allow a detailed check of our predictions.

A much better way to study our predictions systematically occurs when one can vary Δ_A (or Δ_F) and the uniform anisotropy (e.g., g) in the experiment. This has been widely achieved in *random antiferromagnets,* to which we devote the next few paragraphs.

Consider first an alloy of two antiferromagnets with *competing uniaxial anisotropies* (one, with concentration p, has $g>0$, which favors ordering of the S^1 component, while the other has $g<0$, which favors ordering of the remaining $N-1$ components.[23]) Different values of p correspond to different average values of the uniaxial anisotropy g. In the absence of any additional random terms, Fishman and Aharony[23] predicted the phase diagram shown in Fig. 15(a). A tetracritical point occurs when $g=0$, in which case all the N components are expected to order simultaneously. Indeed, such a phase diagram was recently observed[24] in $Fe_pCo_{1-p}Cl_2\cdot 6H_2O$. However, the similar system $Fe_pCo_{1-p}Cl_2$ represented a more complicated situation: Wong *et al.*[25] observed the existence of random off-diagonal coupling terms of the type S^1S^i $(i>1)$, which create random fields on the S^1 component when S^i orders (and vice versa) thus replacing the "mixed" phase by one of domains (for $N-1=2$).

In the absence of any uniform anisotropy terms, random off-diagonal coupling terms like S^iS^j $(i\neq j)$ should destroy long-range order both for the $N-1$ transverse components $N\geq 3$ and for all the N components that order at the tetracritical point. These would be replaced by spin-glass phases, as in our Fig. 5(b). The transverse phase is probably stabilized by higher-order uniform (e.g., cubic) anisotropy terms, which must be relatively strong in order also to show no first-order effects. Intermediate values of the cubic anisotropy might yield a spin-glass phase between the paramagnetic one and the transverse one, as shown schematically in Fig. 15(b). Various other possibilities might occur for various strengths of the cubic term, and it would be of interest to study the full T-g-v-Δ_A phase diagram.

Another way to vary g for antiferromagnets is to apply a uniform magnetic field, as was done for *metamagnets.*[26] In the random case, the magnetic field generates local random staggered fields,[27] which complicate the studies of the Ising transition into the longitudinal phase.[28] In addition, off-diagonal random terms like S^1S^i will immediately generate random fields on the transverse phase, and lead to the same discussion as above.

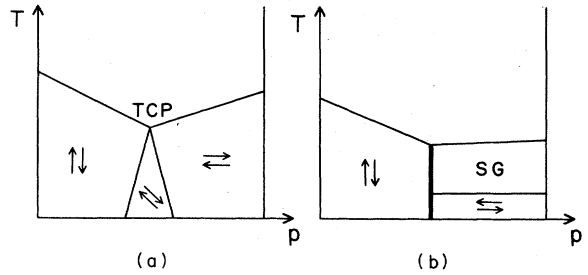

FIG. 15. Schematic phase diagram for antiferromagnets with mixed anisotropies. TCP is the tetracritical point. (a) Case without random off-diagonal couplings. (b) Case with random off-diagonal couplings and intermediate cubic anisotropy (thick line denotes a first-order transition).

Our discussion here has ignored several effects which might lead to further complications. First, we described the transition into the longitudinal Ising phase as if it were a "standard" simple transition. As realized recently,[28] even at $d=3$ the random fields cause complicated slow relaxation phenomena, and the monodomain-ordered equilibrium phase may never be reached in realistic experiments. Similar metastability difficulties may occur in all the cases discussed here. Second, we concluded that many of the ordered phases may be reached only via first-order transitions. As explained by Imry and Wortis,[29] randomness may smear first-order transitions, due to a gradual ordering of domains within the system. This smearing may be an additional cause for the apparent lack of discontinuities in the real experiments. These complicated effects, as well as detailed calculations beyond the $N\rightarrow\infty$ limit, are left for future studies.

ACKNOWLEDGMENTS

Y. Y. Goldschmidt acknowledges the hospitality of Tel Aviv University, where this work was carried out. A. Aharony acknowledges the hospitality of the Solid State Theory group at Brookhaven National Laboratory, where this paper was written. The partial support of the U.S.-Israel Binational Science Foundation and the U.S. National Science Foundation under Grant No. DMR-84-41496 is also gratefully acknowledged.

APPENDIX A

In this appendix we derive the expression for the free energy of the random-anisotropy model in the large-N limit. Starting with the replicated Hamiltonian (5.2), all couplings except m_0^2, u, and Δ_A set equal to zero, and we have

$$F=\lim_{n\rightarrow 0}\frac{1}{n}\left[\int[dS_\alpha^i]\exp\left[-\int\mathscr{H}d^dx\right]-1\right]. \quad \text{(A1)}$$

Introducing collective fields $Q^{\alpha\beta}$ $(\alpha\neq\beta)$ and X^α we have

$$F=\lim_{n\to 0}\frac{1}{n}\left\{\int [dX^{\alpha}][dQ^{\alpha\beta}][d\sigma_{\alpha}]\prod_{i\geq 2}[dS^{i}_{\alpha}]\exp\left[-\int d^{d}x\left\{\frac{N}{2}\sum_{\alpha}[X^{\alpha}(x)]^{2}+\frac{N}{24}\Delta\sum_{\alpha\neq\beta}[Q^{\alpha\beta}(x)]^{2}\right.\right.\right.$$
$$+\tfrac{1}{2}\sum_{\alpha,\beta}S^{i}_{\alpha}(x)(\{-\partial^{2}+m_{0}^{2}-i[(u-\Delta)/3]^{1/2}X^{\alpha}(x)\}\delta^{\alpha\beta}-\Delta Q^{\alpha\beta}(x)/6)S^{i}_{\beta}(x)$$
$$\left.\left.\left.+\tfrac{1}{2}\sum_{\alpha,\beta}\sigma_{\alpha}(x)(\{-\partial^{2}+m_{0}^{2}-i[(u-\Delta)/3]^{1/2}X^{\alpha}(x)\}\delta^{\alpha\beta}-\Delta Q^{\alpha\beta}(x)/6)\sigma_{\beta}(x)-H\sum_{\alpha}\sigma_{\alpha}(x)\right\}\right]-1\right\}, \quad \text{(A2)}$$

where σ stands for the longitudinal component S^{1} and we have introduced a magnetic field in the 1 direction. The fields S^{i}_{α} with $i\geq 2$ can now be separated out using the formula

$$\int\prod_{i\geq 2}[dS^{i}_{\alpha}]\exp\left[-\int d^{d}x\sum_{i}\sum_{\alpha,\beta}S^{i}_{\alpha}A_{\alpha\beta}S^{i}_{\beta}\right]$$
$$=\exp\left[-\frac{N}{2}tr\ln A\right] \quad \text{(A3)}$$

with

$$A_{\alpha\beta}=\tfrac{1}{2}(\{-\partial^{2}+m_{0}^{2}-i[(u-\Delta)/3]^{1/2}X^{\alpha}\}\delta^{\alpha\beta}-\Delta Q^{\alpha\beta}/6)\ . \quad \text{(A4)}$$

Assuming now that $\langle\sigma\rangle\sim\sqrt{N}$ the large-N limit amounts to a saddle point of the free energy. We assume that at the saddle point

$$X^{\alpha}=X\ , \quad \text{(A5)}$$
$$Q^{\alpha\beta}=q\ , \quad \text{(A6)}$$
$$\sigma^{\alpha}=M\ , \quad \text{(A7)}$$

independent of α and β and we obtain

$$\frac{F}{N}=\tfrac{1}{2}X^{2}-\tfrac{1}{24}\Delta q^{2}$$
$$-\tfrac{1}{12}\Delta q\int_{p}\frac{1}{p^{2}+m_{0}^{2}-i[(u-\Delta)/3]^{1/2}X+\Delta q/6}$$
$$+\tfrac{1}{2}\int_{p}\ln\{p^{2}+m_{0}^{2}-i[(u-\Delta)/3]^{1/2}X+\Delta q/6\}$$
$$+\tfrac{1}{2}M^{2}\{m_{0}^{2}-i[(u-\Delta)/3]^{1/2}X+\Delta q/6\}-HM\ . \quad \text{(A8)}$$

Putting

$$\Sigma=m_{0}^{2}-i[(u-\Delta)/3]^{1/2}X+\Delta q/6\ , \quad \text{(A9)}$$

we arrive at Eq. (6.9) where we have also added the contribution $-vM^{4}$ due to cubic symmetry breaking.

APPENDIX B

In this appendix we consider the free energy in Eq. (6.11) in the case $t=0$, $d=3$. The spin-glass solution of the equation of state (with $d=3$) is given by

$$\Sigma=\tfrac{1}{36}f_{2}^{2}\Delta^{2},\quad q=\tfrac{1}{6}f_{1}f_{2}\Delta,\quad M=0 \quad \text{(B1)}$$

and the free energy (putting $u-\Delta\to u$ for small Δ) is

$$F_{1}=\tfrac{1}{3456}f_{1}^{4}\Delta^{3}\left[\frac{1}{3}-\frac{1}{4u}\Delta\right]=\tfrac{1}{3456}f_{1}^{4}\rho^{3}v^{3}\left[\frac{1}{3}-\frac{1}{4u}\rho v\right], \quad \text{(B2)}$$

where we have put $\Delta=\rho v$ and used the fact that $f_{2}=f_{1}/2$ in $d=3$. The ferromagnetic solution is given by

$$M=\tfrac{1}{2}f_{1}[\sqrt{v}+(v-\tfrac{2}{3}f_{2}\Delta/f_{1})^{1/2}]=\tfrac{1}{2}f_{1}\lambda\sqrt{v}\ , \quad \text{(B3)}$$

$$\Sigma=\tfrac{1}{4}f_{1}^{2}\lambda^{2}v^{2},\quad q=\frac{3f_{1}^{3}\lambda^{3}v/4}{3f_{1}\lambda-f_{2}\rho} \quad \text{(B4)}$$

with

$$\lambda=1+(1-\tfrac{2}{3}f_{2}\rho)^{1/2}\ , \quad \text{(B5)}$$

and for this solution one obtains

$$F_{2}=-f_{1}^{4}\lambda^{3}v^{3}\left[\frac{2-\lambda}{48}+\frac{\lambda\rho}{32}\frac{3\lambda^{3}+2\rho-12\lambda}{(6\lambda-\rho)^{2}}\right]$$
$$-\frac{3}{32u}f_{1}^{4}\lambda^{4}v^{4}\left[1-\frac{2\lambda\rho}{18\lambda-3\rho}\right]^{2}. \quad \text{(B6)}$$

As $\rho\to 0$, $\lambda\to 2$ and we see that $F_{1}\to 0$, $F_{2}\to-(3/2u)f_{1}^{4}v^{4}$, so obviously the ferromagnetic solution has lower energy.

On the other hand, as $\rho\to 3f_{1}/2f_{2}$ ($=3$ in three dimensions), $\lambda\to 1$ and we obtain

$$F_{1}=\tfrac{1}{384}f_{1}^{4}v^{3}(1-9v/u)\ , \quad \text{(B7)}$$

$$F_{2}=\tfrac{1}{96}f_{1}^{4}v^{3}(1-v/u)\ , \quad \text{(B8)}$$

so in this case $F_{1}<F_{2}$ and the spin-glass solution is more stable.

[1]Y. Imry and S.-K. Ma, Phys. Rev. Lett. **35**, 1399 (1975).
[2]R. A. Pellcovits, E. Pytte, and J. Rudnick, Phys. Rev. Lett. **40**, 476 (1978); **48**, 1297(E) (1982).
[3]A. Aharony, Solid State Commun. **28**, 667 (1978).
[4]A. Aharony and E. Pytte, Phys. Rev. Lett. **45**, 1583 (1980).
[5]P. Lacour-Gayet and G. Toulouse, J. Phys. (Paris) **35**, 425 (1974).
[6]See also R. M. Hornreich and H. G. Shuster, Phys. Rev. B **26**, 3929 (1982).
[7]S. Edwards and P. W. Anderson, J. Phys. F **5**, 965 (1975).
[8]Y. Y. Goldschmidt, Nucl. Phys. **B225**, 123 (1983).
[9]A. Aharony, Phys. Rev. B **8**, 4270 (1973).
[10]D. R. Nelson, Phys. Rev. B **13**, 2222 (1976).
[11]M. E. Fisher and P. Pfeuty, Phys. Rev. B **6**, 1889 (1984).
[12]A. Aharony, Phys. Rev. B **12**, 1038 (1975).
[13]D. Mukamel and G. Grinstein, Phys. Rev. B **25**, 381 (1982).
[14]A. Arrott and J. N. Noakes, Phys. Rev. Lett. **19**, 786 (1967). The method was discussed in detail by J. S. Kouvel and M. E. Fisher, Phys. Rev. **136**, A1626 (1964).
[15]Figure 3(a) is essentially the same as was obtained to leading order in Δ_F in Ref. 4. To obtain Fig. 3(b) one must sum up all orders in Δ_A (see Ref. 8).
[16]R. A. Pelcovits, Phys. Rev. B **19**, 465 (1979); D. R. Nelson and R. A. Pelcovits, *ibid.* **16**, 2191 (1977); R. A Pelcovits and D. R. Nelson, Phys. Lett. **57A**, 23 (1976).
[17]A. Aharony and E. Pytte, Phys. Rev. B **27**, 5872 (1983).
[18]A. Aharony, in *Phase Transitions and Critical Phenomena,* edited by C. Domb and M. S. Green (Academic, New York, 1976), p. 357.
[19]A. Aharony, Phys. Rev. B **18**, 3318 (1978).
[20]A. D. Bruce and A. Aharony, Phys. Rev. B **11**, 478 (1975).
[21]D. J. Wallace, J. Phys. C **6**, 1390 (1973).
[22]A. Aharony, J. Phys. C **7**, L63 (1974); P. A. Pearce and C. J. Thompson, Prog. Theor. Phys. **55**, 665 (1976).
[23]S. Fishman and A. Aharony, Phys. Rev. B **18**, 3507 (1978).
[24]K. Katsumata, H. Yoshizawa, G. Shirane, and R. J. Birgeneau (unpublished).
[25]P. Wong, P. M. Horn, R. J. Birgeneau, and G. Shirane, Phys. Rev. B **27**, 428 (1983).
[26]E.g., Y. Shapira and N. F. Oliviera, Jr., Phys. Rev. B **27**, 4336 (1983).
[27]S. Fishman and A. Aharony, J. Phys. C **12**, L729 (1979).
[28]R. J. Birgeneau, R. A. Cowley, G. Shirane, and H. Yoshizawa, J. Stat. Phys. **34**, 817 (1984).
[29]Y. Imry and M. Wortis, Phys. Rev. B **19**, 3580 (1979).
[30]See, e.g., S. K. Ma, *Modern Theory of Critical Phenomena* (Benjamin, New York, 1976), and references therein.
[31]F. J. Wegner and A. Houghton, Phys. Rev. A **10**, 435 (1974).
[32]S. Hikami and E. Brezin, J. Phys. A **11**, 1141 (1978).
[33]E. Brezin, J. Zinn-Justin, and J. C. LeGuillou, Phys. Rev. B **14**, 4976 (1976); Phys. Rev. D **14**, 2615 (1976).